applied biosciences

MDPI

Article

In Silico Ligand Docking Approaches to Characterise the Binding of Known Allosteric Modulators to the Glucagon-Like Peptide 1 Receptor and Prediction of ADME/Tox Properties

Chiemela S. Odoemelam [1], Elena Hunter [1], John Simms [2], Zeeshan Ahmad [3], Ming-Wei Chang [4], Benita Percival [3], Ian H. Williams [5], Marco Molinari [6], Shina Caroline Lynn Kamerlin [7] and Philippe B. Wilson [1,*]

[1] School of Animal, Rural and Environmental Sciences, Brackenhurst Campus, Nottingham Trent University, Nottingham NG25 0QF, UK; chiemela.odoemelam@ntu.ac.uk (C.S.O.); elena.hunter@ntu.ac.uk (E.H.)
[2] School of Life and Health Sciences, Aston University, Aston Triangle, Birmingham B4 7ET, UK; j.simms3@aston.ac.uk
[3] Faculty of Health and Life Sciences, De Montfort University, The Gateway, Leicester LE1 9BH, UK; zahmad@dmu.ac.uk (Z.A.); benita.percival@ntu.ac.uk (B.P.)
[4] Nanotechnology and Integrated Bioengineering Centre, Jordanstown Campus, University of Ulster, Newtownabbey BT37 0QB, UK; m.chang@ulster.ac.uk
[5] Department of Chemistry, University of Bath, Bath BA1 7AY, UK; i.h.williams@bath.ac.uk
[6] School of Applied Sciences, University of Huddersfield, Huddersfield HD1 3DH, UK; m.molinari@hud.ac.uk
[7] Department of Chemistry—BMC, Uppsala University, BMC Box 576, 751 23 Uppsala, Sweden; lynn.kamerlin@kemi.uu.se
* Correspondence: philippe.wilson@ntu.ac.uk

check for updates

Citation: Odoemelam, C.S.; Hunter, E.; Simms, J.; Ahmad, Z.; Chang, M.-W.; Percival, B.; Williams, I.H.; Molinari, M.; Kamerlin, S.C.L.; Wilson, P.B. In Silico Ligand Docking Approaches to Characterise the Binding of Known Allosteric Modulators to the Glucagon-Like Peptide 1 Receptor and Prediction of ADME/Tox Properties. *Appl. Biosci.* **2022**, *1*, 143–162. https://doi.org/10.3390/applbiosci1020010

Academic Editor: Alfonso Zambon

Received: 31 May 2022
Accepted: 29 July 2022
Published: 2 August 2022

Publisher's Note: MDPI stays neutral with regard to jurisdictional claims in published maps and institutional affiliations.

Copyright: © 2022 by the authors. Licensee MDPI, Basel, Switzerland. This article is an open access article distributed under the terms and conditions of the Creative Commons Attribution (CC BY) license (https://creativecommons.org/licenses/by/4.0/).

Abstract: The glucagon-like peptide 1 receptor (GLP-1R) is a member of the family (or class) B G-protein-coupled receptor (GPCR). The receptor is a regulator of insulin and a key target in treating Type 2 diabetes mellitus. In this investigation, computational chemistry techniques such as molecular docking were combined with in silico ADME/Tox predictions to determine the position and structure of the allosteric binding site, as well as to examine how the allosteric modulators bind to the binding site. In silico evaluation was used to evaluate the ADME/Tox properties of the allosteric modulators. The findings of the ligand docking studies suggest that the allosteric binding site is situated around the transmembrane (TM) domain TM 6 of the receptor in the active state. ADME/Tox characterisation of the allosteric modulators demonstrate that compounds **1**–**3** (2,6,7-trichloro-3-(trifluoromethyl)quinoxaline, 1-(5-(4-(tert-butyl)phenyl)-1,3,4-oxadiazol-2-yl)-6,6-dimethyl-3-(methylsulfonyl)-6,7-dihydrobenzo[c]thiophen-4(5H)-one, 2-((4-chlorophenyl)thio)-3-(trifluoromethyl)quinoxaline, respectively) complied with the traditional method of evaluating drug-likeness; Lipinski's rule of 5. The allosteric modulator compound **4** (3-(8-chloro-6-(trifluoromethyl) imidazo[1,2-a]pyridin-2-yl)phenyl cyclohexanecarboxylate) failed to comply with Lipinski's rule of five as a result of having a logP value of over 5.6. Moreover, molecular docking studies provide insights into potential allosteric binding sites and possible interactions. Finally, the in silico ADME/Tox study results are described as relevant to developing a viable drug candidate.

Keywords: ADME/Tox; GLP-1R; ligand binding; allosteric binding site; allosteric modulator; GPCR

1. Introduction

Glucagon-like peptide1 receptor (GLP-1R) is of particular interest due to its role in the treatment of type 2 diabetes mellitus (T2D) and appetite regulation [1]. This receptor belongs to the small family (or class) B of G-protein-coupled receptors (GPCRs), which consist structurally of seven transmembrane (TM) domains of 310–420 residues, interconnected by three intracellular (IL) and extracellular (EL) loops, and an extracellular N-terminal domain (NTD) of 120–160 residues (Figure 1) [2,3].

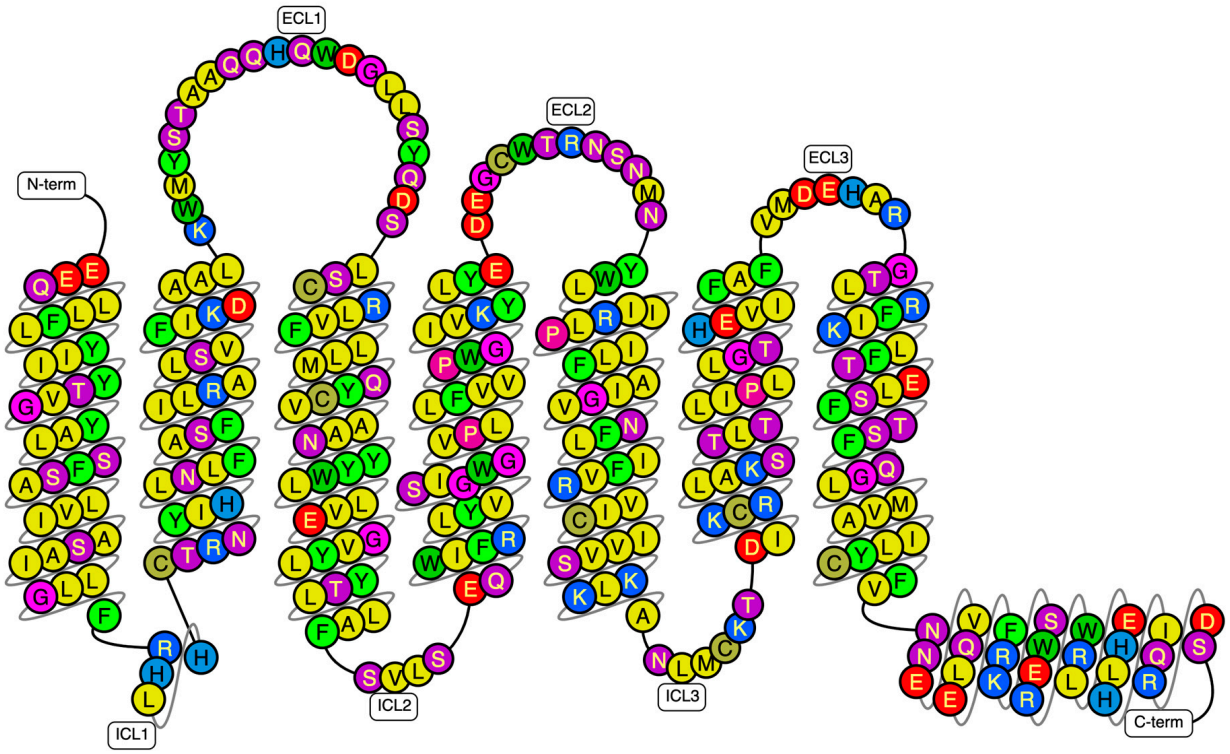

Figure 1. A schematic representation of GLP-1R showing the transmembrane domains, the N- and C-termini, and the intracellular and extracellular loops generated using G-protein-coupled receptor (GPCR) database tools. Adapted from Refs. [4,5].

Glucagon-like peptide 1 (GLP-1) is the endogenous ligand of GLP-1R. In response to food intake, it is produced from the gastrointestinal tract and has vital roles in regulating insulin secretion, appetite control, and carbohydrate metabolism [6]. As a result of the distinctive processing of its precursor glucagon, GLP-1 occurs in two active forms: GLP-1 (7–37 amide) and GLP-1 (7–36 amide). GLP-1 (7–36 amide) is the primary circulatory form, which exerts insulinotropic and glucoregulatory functions. However, within 1 to 4 min of secretion, both active forms are degraded by dipeptidyl peptidase 4 (DPP-IV) through cleavage of NH2-terminal amino acids to their respective principal metabolites; 9–37 amide and 9–36 amide (Figure 2), of which each remains in circulation for about 30 min [7]. Contrary to the antecedent belief that GLP-1 (9–36 amide) is pharmacologically inactive as a result of its weak or no insulinotropic activity, recent findings have demonstrated that GLP-1 (9–36 amide) possess distinctive extra-pancreatic insulin-like actions in the heart, liver and vasculature, which are autonomously mediated irrespective of the GLP-1R [8–11]. GLP-1 (7–36 amide) is a 30-amino-acid peptide hormone released from intestinal L-cells following supplement ingestion [12]. The peptide GLP-1 has numerous functions, including potentiation of the glucose-actuated release of insulin from pancreatic beta cells, heightening insulin articulations, obstruction of beta-cell apoptosis, progression of beta-cell neogenesis, diminishing glucagon emission, conceding gastric discharging, supporting satiety, and intensifying peripheral glucose disposal. It is thus also a physiological regulator of appetite and food intake [13].

Fasting blood concentration of GLP-1 (9–36 amide) in humans usually ranges from 5 to 15 pmol/L, and there is usually a two- to four-fold increase after ingesting food. There is an increase in blood GLP-1 concentration 15 min after food ingestion, and peak concentration is reached after 60 min. The blood GLP-1 concentration decreases gradually in the second hour until the next time food is ingested [7]. It is clear from these varied activities that GLP-1 plays a central role in controlling postprandial glucose levels and, in that capacity, drugs that stimulate the GLP-1 receptor, such as dipeptidyl peptidase 4 inhibitors or GLP-1 analogues, have been manufactured for use in the treatment of type 2 diabetes

mellitus (T2D) [14,15]. The excessive secretion of GLP-1 has been hypothesised to be responsible for postprandial reactive hypoglycaemia, while diminished secretion might lead to obesity [12]. T2D treatment needs the positive allosteric modulation of GLP-1R to inhibit glucagon secretion, thus stimulating insulin secretion in a glucose-dependent routine [16]. A structural study carried out by Song et al. [16] showed similarity in the transmembrane domain (TMD) architecture of GLP-1R and Glucagon receptor (GCGR), which was also consistent with the overlap in their primary sequences (45% similar in their TMDs). The human GLP-1R TMD was crystallised with two negative allosteric modulators, NNC0640 and PF-06372222, respectively, at 3.0 and 2.7 Å resolution. The crystallised structures of GLP-1R and GCGR showed a common binding pocket for the negative allosteric modulators, which is located outside helices V–VII, close to the receptor's intracellular domain [16]. A molecular-modelling and mutagenesis study has shown that agonist positive allosteric modulators also target the same region but in a clear-cut sub-pocket at the interface between helices V and VI, which may aid the formation of an intracellular binding site that enhances G-protein coupling [16]. The secretin receptors have immense potential in drug discovery due to their importance in fundamental homeostatic functions. To date, three of these hormones are used clinically: glucagon, parathyroid hormone and calcitonin, for the treatment of hypoglycaemia, osteoporosis, and hypercalcaemia, respectively [17]. This study aims to determine the allosteric binding site and molecular mechanism of allosteric binding to GLP1-R, using allosteric modulators identified through a literature survey. We also perform in silico evaluation of the ADME/Tox properties of the allosteric modulators.

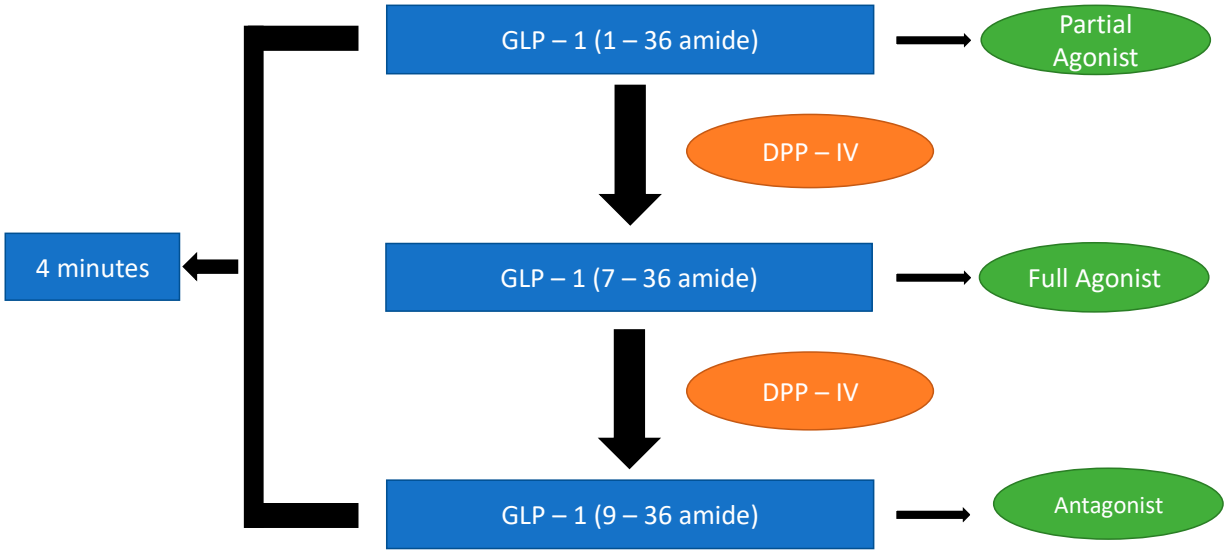

Figure 2. Illustration showing the breakdown of three forms of GLP-1 (1–36 amide) by DPP-IV at different time intervals. DPP-IV is depicted in Orange and GLP-1 in blue. The green ovals show the forms of GLP-1 and their characteristic when degraded by DPP-IV. (It shows if that form is an agonist/antagonist to the GLP-1R).

2. Computational Methods

2.1. Selection of Ligands and Receptors

Four known positive allosteric modulators of GLP-1R were selected for this study because of their GLP-1R activating activity, as reported by Bueno et al. [18]; these are 1: 2,6,7-trichloro-3-(trifluoromethyl)quinoxaline, 2: 1-(5-(4-(tert-butyl)phenyl)-1,3,4-oxadiazol-2-yl)-6,6-dimethyl-3-(methylsulfonyl)-6,7-dihydrobenzo[c]thiophen-4(5H)-one, 3: 2-((4-chlorophenyl)thio)-3-(trifluoromethyl)quinoxaline and 4: 3-(8-chloro-6-(trifluoromethyl) imidazo[1,2-a]pyridin-2-yl)phenyl cyclohexanecarboxylate (Figure 3). These structures were drawn using ChemDraw version 18.0 (PerkinElmer Informatics, Inc). The crystallographic coordinates of the active and inactive GLP-1R structures were obtained from the

protein data bank with the following PDB IDs: 5VAI (resolution: 4.1 Å) [19] (active), 5VEW (resolution: 2.7 Å) [16] (inactive) and 6B3J (resolution: 3.3 Å) [20] (active). Newer structures of the GLP-1R (PDB IDs: 6KJV (resolution: 2.8 Å) [21], 6VCB (resolution: 3.3 Å) [22], 6XOX (resolution: 3.1 Å) [23]) have been crystallised using methods such as electron microscopy and x-ray diffraction. These newer structures differ from the crystal structures used in this study and from each other in terms of the ligand bound for the crystallisation, method of crystallisation, and resolution (Table S1 in the Supplementary).

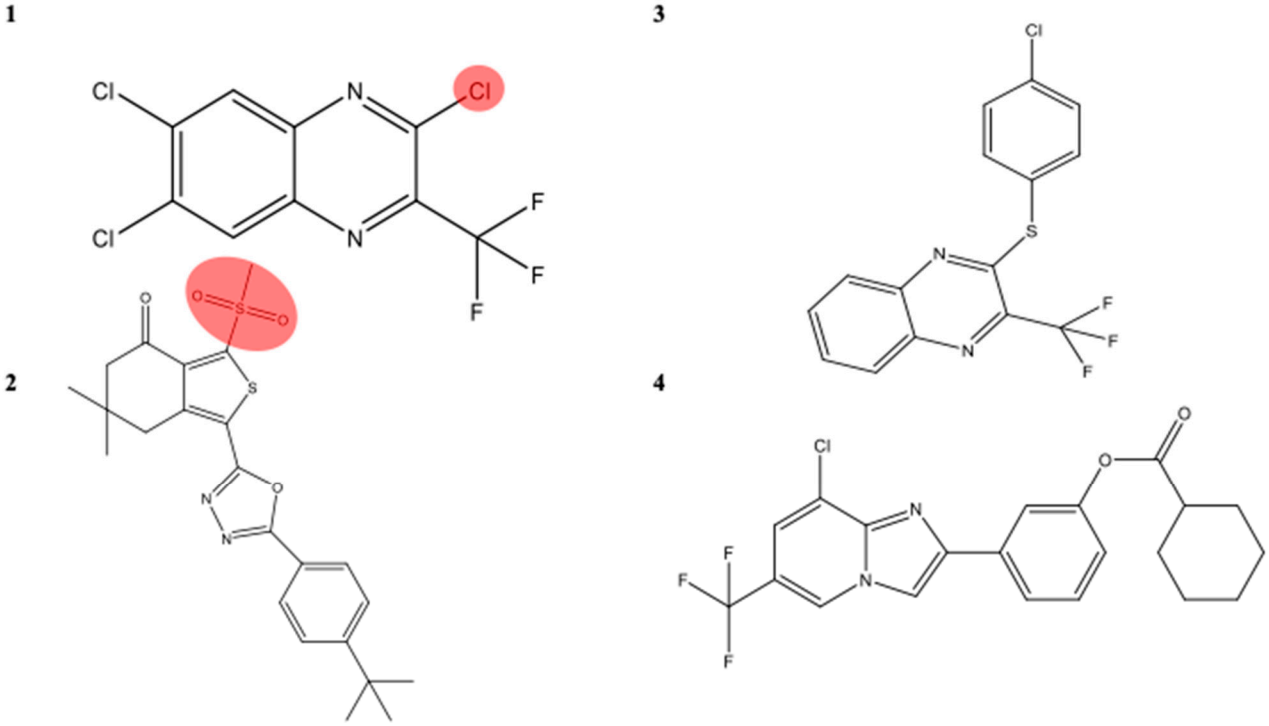

Figure 3. Chemical structures of known Glucagon-like peptide 1 receptor allosteric modulators. Adopted from Bueno et al. [18]. The groups which leave in a nucleophilic attack in compounds **1** and **2** are shaded in red. 1: 2,6,7-trichloro-3-(trifluoromethyl)quinoxaline (Compound, EC50 Wildtype (WT) (S.D., n) 4700 (1000, 4) nm) [18], 2: 1-(5-(4-(tert-butyl)phenyl)-1,3,4-oxadiazol-2-yl)-6,6-dimethyl-3-(methylsulfonyl)-6,7-dihydrobenzo[c]thiophen-4(5H)-one (Compound, EC50 Wildtype (WT) (S.D., n) 1500 (1000, 4) nm) [18], 3: 2-((4-chlorophenyl)thio)-3-(trifluoromethyl)quinoxaline (Compound, EC50 Wildtype (WT) (S.D., n) >30,000 (NA, 4) nm) [18], 4: 3-(8-chloro-6-(trifluoromethyl)imidazo[1,2-a]pyridin-2-yl)phenyl cyclohexanecarboxylate (Compound, EC50 Wildtype (WT) (S.D., n) >30,000 (NA, 4) nm) [18].

2.2. Ligand and Receptor Preparation, Molecular Docking, and Binding Affinity Analysis

Ligand docking into the active (PDB IDs: 5VAI [19], 6B3J [20]-Chain R) and the inactive (PDB ID: 5VEW [16]-Chain A) structures of the GLP-1R crystal structures was performed using Flare, version 5.0 (Cresset Software, Litlington, UK). The protein and ligand structures were prepared using the Flare software default settings (the full preparation of the protein and ligand at a pH of 7.0 and active site size of 6.00 Å adds missing hydrogens to proteins and cofactors and assigns optimal ionization states to the protein residues. It optimises the spatial positions of polar hydrogen atoms to maximise hydrogen bonding and minimise steric clashes. The side chain orientation of His, Asn and Gln are optimized, then the residues with unsolved side chains are detected and reconstructed). The protein and ligands were minimized using the XED accurate method on Flare. The very accurate but slow option for the docking calculation was selected (this method is based on the genetic algorithm, and it performs three independent docking runs to achieve the lowest calculated binding energy). The grid box was set by picking amino acid residues present in the

protein's TM5, TM6 and TM7. The poses with the highest binding energy were selected and visualised using BIOVIA Discovery Studio Visualiser, version 19.1 (Dassault Systems, San Diego, CA, USA).

The binding affinity of the protein–ligand complexes was analysed using the PRODIGY web server [24,25].

2.3. In Silico ADME/Tox Prediction

In silico ADMET studies were performed using the ADMET predictor v.9.5 (Simulations Plus, Inc., Lancaster, CA, USA). The SMILES code of the compounds was uploaded into the software for evaluations. The ADMET properties were calculated at pH 7.4, evaluating the compounds' physicochemical, metabolic, and toxicity properties.

3. Results

3.1. Interaction of 2,6,7-Trichloro-3-(trifluoromethyl)quinoxaline (Compound **1***) with the GLP-1 Receptor*

The findings of the in silico allosteric modulators docking studies showed compound 1 being juxtaposed to TM6 of the active structure with PDB ID: 5VAI [19] (binding energy −6.46 Kcal/mol) (Figure 4A), TM7 of the inactive structure with PDB ID: 5VEW [16] (binding energy −8.50 Kcal/mol) (Figure 4B), and both TM6 of the active structure with PDB ID: 6B3J [20] (binding energy −6.70 Kcal/mol) (Figure 4C). In poses 2 and 3 of the 5VAI-Compound **1** complex, the ligand docked at the TM6 of the receptor with binding energies of 6.34 Kcal/mol and 6.25 Kcal/mol respectively. In the pose 2 of the 5VEW-Compound **1** complex (binding energy −8.18 Kcal/mol) the ligand docked at the TM6 of the allosteric binding site. In the third pose, the ligand juxtaposed at TM7 of the receptor (binding energy −6.26 Kcal/mol). In the 6B3J-Compound **1** complex, the ligand was bound to the TM6 of the receptor with bindings energies of −6.59 Kcal/mol and −6.43 Kcal/mol for poses 2 and three respectively. A 2D schematic of the allosteric modulators' protein–ligand interaction and respective receptors is presented (Figure 5). A summary of the amino acids interacting with the ligand at the allosteric binding site is presented in Tables 1, S3 and S4.

Table 1. Table showing amino acids interacting in the binding sites with compound **1**.

S/N	5VAI	5VEW	6B3J
1	LEU 354	ARG 348	LEU 354
2	THR 355	TYR 402	ILE 357
3	PRO 358	VAL 405	GLN 394
4	ILE 357	LYS 351	HIS 363
5	PHE 390	LEU 349	PHE 393
6	MET 397	HIS 180	MET 397
7	LEU 401		PRO 358
8	LYS 351		PHE 390

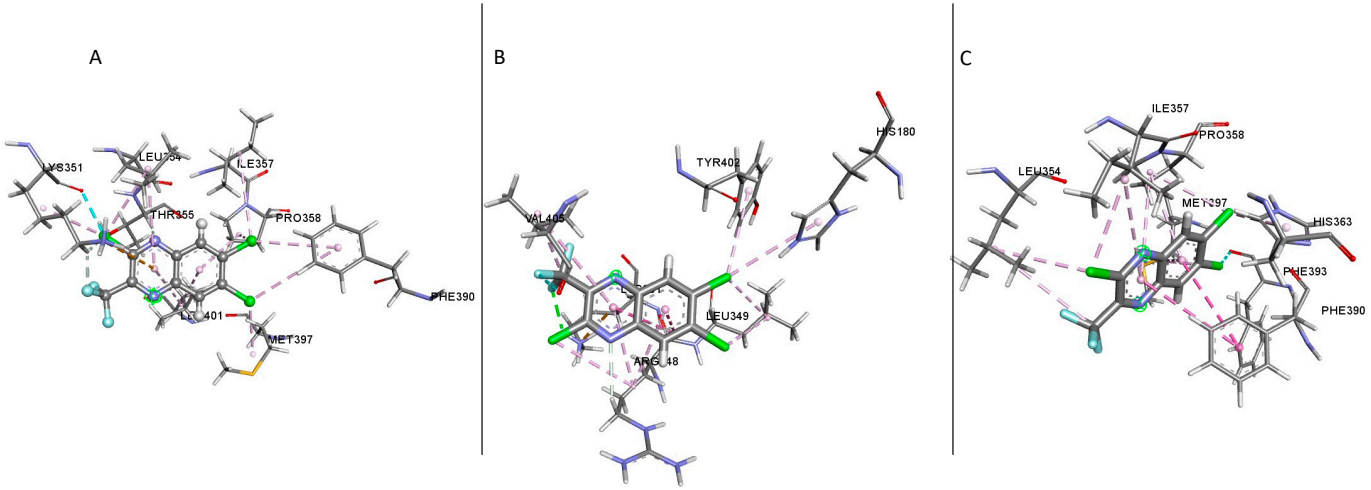

Figure 4. Schematic showing ligand—GLP-1R complexes. (**A**) 1:5VAI, (**B**) 1:5VEW, (**C**) 1:6B3J.

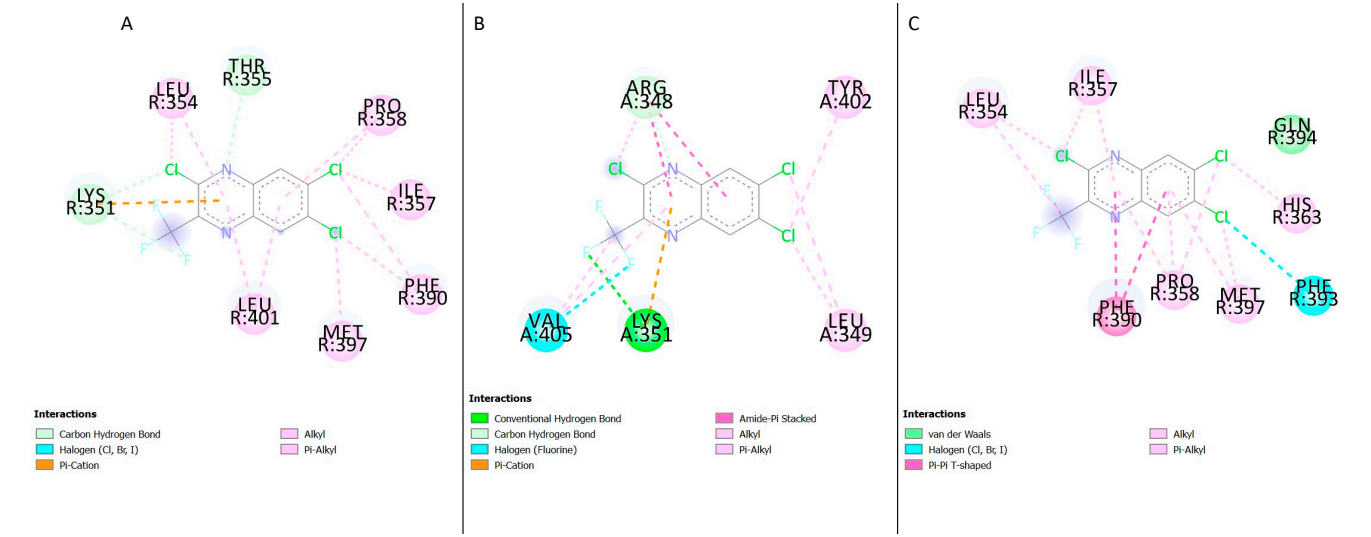

Figure 5. The protein–ligand interaction between compound **1** and the GLP 1 receptor generated using BIOVIA Discovery Studio Visualiser. (**A**) 1:5VAI, (**B**) 1:5VEW, and (**C**) 1:6B3J.

3.2. Interaction of 1-(5-(4-(Tert-butyl)phenyl)-1,3,4-oxadiazol-2-yl)-6,6-dimethyl-3-(methylsulfonyl)-6,7-dihydrobenzo[c]thiophen-4(5H)-one (Compound **2***) with the GLP-1 Receptor*

Ligand docking studies were performed to understand the binding of 1-(5-(4-(tert-butyl)phenyl)-1,3,4-oxadiazol-2-yl)-6,6-dimethyl-3-(methylsulfonyl)-6,7-dihydrobenzo[c] thiophen-4(5H)-one (compound **2**) to the active (PDB IDs: 5VAI and 6B3J) and inactive (5VEW) of GLP-1R structures. The showed compound **2** being juxtaposed to TM6 of 5VAI [19] (binding energy −7.55 Kcal/mol) (Figure 6A), to TM6 of 5VEW [16] (binding energy −7.189 Kcal/mol) (Figure 6B), and TM6 of 6B3J (binding energy −7.67 Kcal/mol) (Figure 6C). In the other poses analysed the ligand docked at the TM6 of all the GLP1R structure used for this study (5VAI, pose 2 binding energy (−7.45 Kcal/mol) and pose 3 binding energy (−7.37 Kcal/mol); 6B3J, pose 2 binding energy (−7.59 Kcal/mol) and pose 3 binding energy (−7.45 Kcal/mol); 5VEW, pose 2 binding energy (−7.066 Kcal/mol) and pose 3 binding energy (−6.873 Kcal/mol). A 2D schematic of the protein–ligand interaction of the allosteric modulators and respective receptors are presented in Figure 7A–C. The amino acid residues interacting with the ligand in the binding site of compound **2** can be observed in Tables 2, S5 and S6.

Table 2. Amino acids which interact in the binding sites with compound **2**.

S/N	5VAI	5VEW	6B3J
1	MET 397	LEU 359	ASN 407
2	PHE 390	PHE 324	ASN 406
3	THR 355	PHE 321	TYR 402
4	LEU 354	PHE 347	LEU 401
5	ILE 357	LEU 354	ARG 176
6		ILE 328	LEU 251
7		PRO 358	HIS 180
8			TYR 250

3.3. Interaction of 2-((4-Chlorophenyl)thio)-3-(trifluoromethyl)quinoxaline (Compound **3***) with the GLP-1 Receptor*

Docking studies carried out for the GLP-1R crystal structures showed compound **3** being juxtaposed to a pocket behind TM6 in 5VAI (binding energy 6.44 Kcal/mol) (Figure 8A), in the inactive structure (5VEW), it juxtaposed to TM6 of the receptor (binding energy 7.877 Kcal/mol) (Figure 8B), in the other active structure (6B3J), compound **3** juxtaposed at TM6 (binding energy −7.27 Kcal/mol). A 2D schematic of the ligands' protein–ligand interaction and respective receptors is presented (Figure 9). In poses 2 and 3 of the 5VAI-Compound **3** complex, the ligand docked at the TM6 of the receptor with binding energies of 6.31 Kcal/mol and 6.28 Kcal/mol respectively. In the pose 2 of the 5VEW-Compound **3** complex (binding energy −6.86 Kcal/mol) the ligand docked at the TM6 of the allosteric binding site. In the third pose, the ligand juxtaposed at TM6 of the receptor (binding energy −6.82 Kcal/mol). In the 6B3J-Compound **3** complex, the ligand was bound between TM6 and TM7 (pose 2) of the receptor with binding energy of −7.12 Kcal/mol. In pose 3 the ligand bound to TM7 of the receptor (binding energy −6.92 Kcal/mol). Table 3 below shows the amino acid residues interacting in the binding sites with compound **3**. Tables S7 and S8 shows amino acid residues interacting with compound **3** in poses 2 and 3.

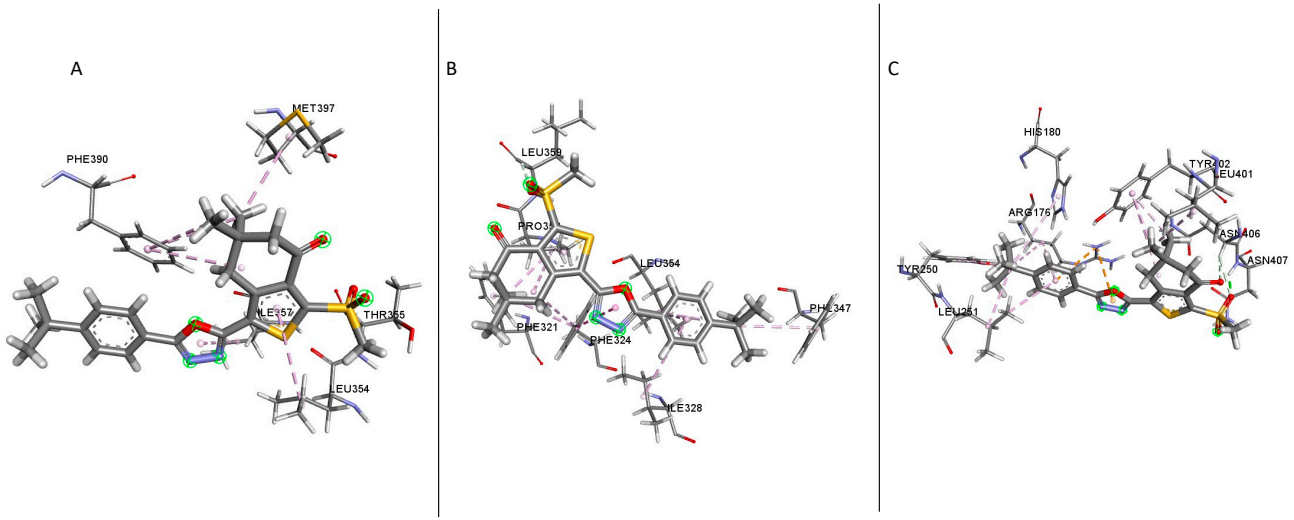

Figure 6. Schematic showing ligand—GLP-1R complexes. (**A**) 2:5VAI, (**B**) 2:5VEW, (**C**) 2:6B3J.

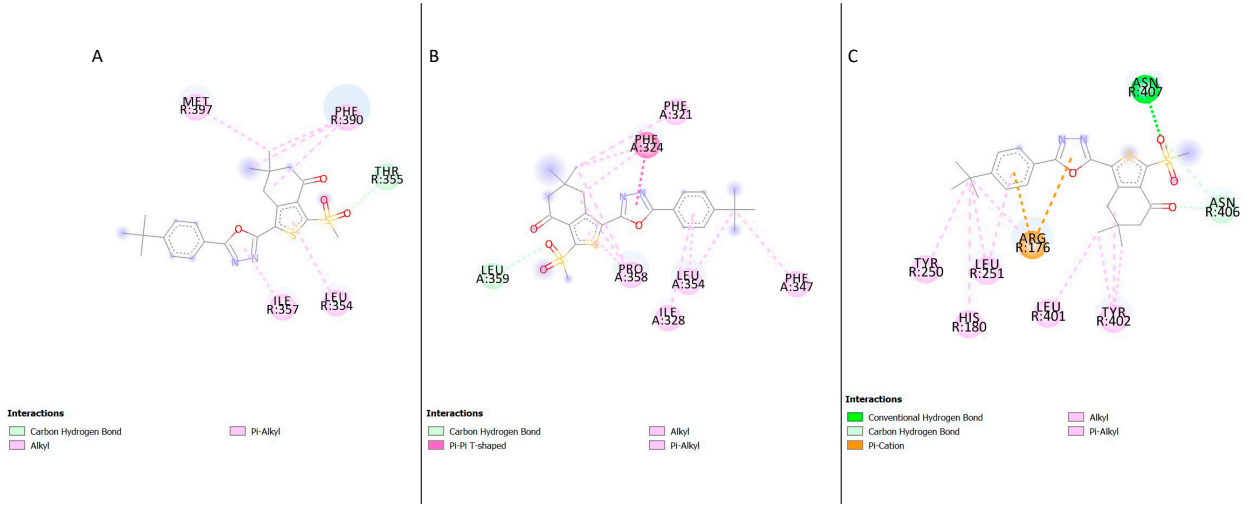

Figure 7. The protein–ligand interaction between compound **2** and the GLP 1 receptor generated using BIOVIA Discovery Studio Visualiser. (**A**) 2:5VAI, (**B**) 2:5VEW, and (**C**) 2:6B3J.

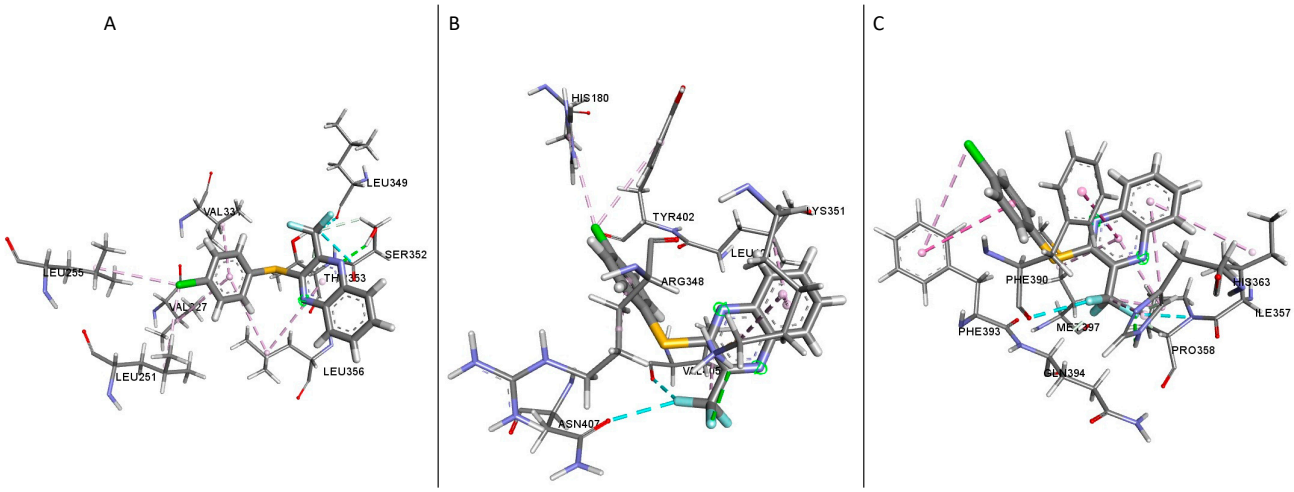

Figure 8. Schematic showing ligand—GLP-1R complexes. (**A**) 3:5VAI, (**B**) 3:5VEW, (**C**) 3:6B3J.

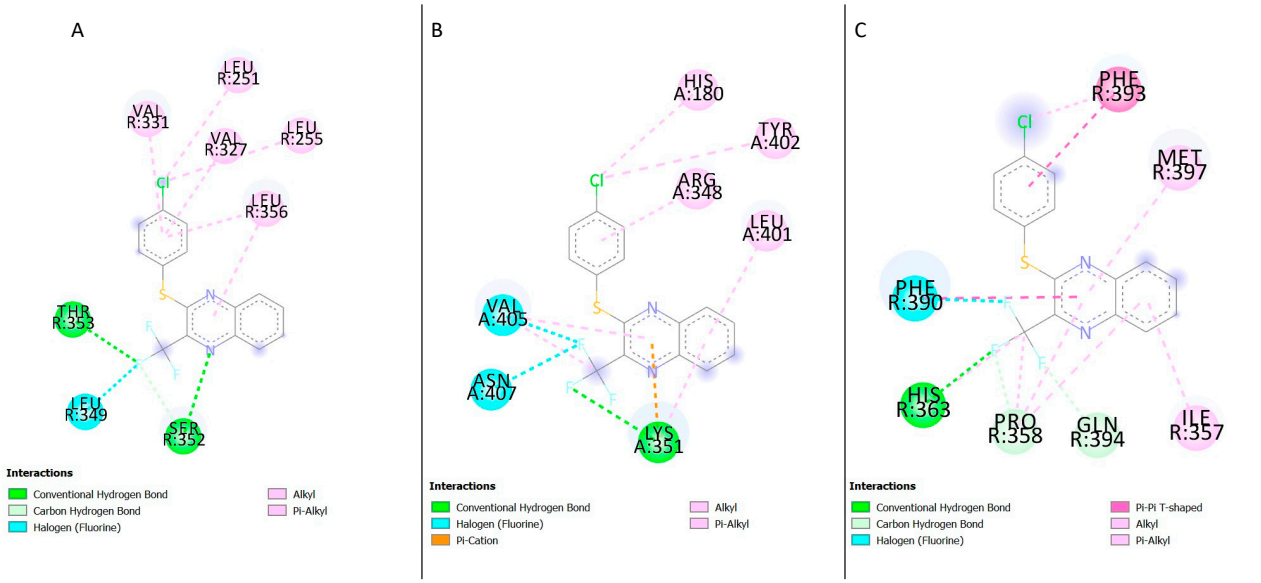

Figure 9. The protein–ligand interaction between compound **3** and the GLP 1 receptor generated using BIOVIA Discovery Studio Visualiser. (**A**) 3:5VAI, (**B**) 3:5VEW, and (**C**) 3:6B3J.

Table 3. Amino acids present in the binding sites for compound **3**.

S/N	5VAI	5VEW	6B3J
1	VAL 331	HIS 180	PHE 393
2	LEU 251	TYR 402	MET 397
3	VAL 327	ARG 348	ILE 357
4	LEU 255	LEU 401	GLN 394
5	LEU 356	LYS 351	PRO 358
6	SER 352	ASN 407	HIS 363
7	LEU 349	VAL 405	PHE 390
8	THR 353		

*3.4. Interaction of 3-(8-Chloro-6-(trifluoromethyl)imidazo[1,2-a]pyridin-2-yl)phenyl Cyclohexanecarboxylate (Compound **4**) with the GLP-1 Receptor*

Ligand docking studies were performed to understand how 3-(8-chloro-6-(trifluoromethyl) imidazo[1,2-a]pyridin-2-yl)phenyl cyclohexanecarboxylate (compound **4**) binds to active (5VAI [19] and 6B3J [20]) and inactive (5VEW [16]) GLP-1R structures. The findings showed four being juxtaposed to TM6 in 5VAI (binding energy −7.25 Kcal/mol) (Figure 10A), to

TM6 in 5VEW (binding energy −9.48 Kcal/mol) (Figure 10B) and TM6 and TM7 in 6B3J (binding energy −7.95 Kcal/mol) (Figure 10C). In the other poses, the ligand docked at the TM6 of the active GLP1R structure was used for this study (5VAI, pose 2 binding energy (−7.159 Kcal/mol) and pose 3 binding energy (−7.157 Kcal/mol); 6B3J, pose 2 binding energy (−7.77 Kcal/mol) and pose 3 binding energy (−7.73 Kcal/mol)). In the inactive structure 5VEW, the ligand docked at TM6 in the second pose (binding energy −9.27 Kcal/mol) and in pose 3, compound **4** juxtaposed between TM6 and TM7 (binding energy −8.22 Kcal/mol). A 2D schematic of the protein–ligand interaction of the ligands and respective receptors are presented in Figure 11A–C. Table 4 below shows the amino acid residues interacting in the binding sites with compound **4**. Tables S7 and S8 show amino acid residues interacting with compound **4** in poses 2 and 3.

Table 4. Amino acids present in the binding site for compound **4**.

S/N	5VAI	5VEW	6B3J
1	THR 355	PHE 393	ILE 366
2	LEU 401	PHE 390	ILE 357
3	PRO 358	LEU 360	PRO 358
4	PHE 390	MET 397	MET 397
5	MET 397	LEU 359	LEU 401
6	LEU 354	GLN 394	ILE 400
7	ILE 357	HIS 363	LEU 354

3.5. Binding Affinity Analysis

Binding affinity analysis is used to measure the strength of biomolecular interactions. The binding affinity of any complex in thermodynamic terms is crucial in determining the feasibility of an interaction occurring in a cell or not at specified conditions [24,26]. The findings of the binding affinity analysis of the protein–ligand complexes analysed using PRODIGY-LIG webserver are shown in the table below (Table 5).

Table 5. Binding affinities of the docked complexes of GLP-1R and the ligands.

Complexes	Binding Affinity ΔGnoelec (Kcal/mol)
5VAI-Compound **1**	−6.8
5VEW-Compound **1**	−7.2
6B3J-Compound **1**	−7.2
5VAI-Compound **2**	−8.5
5VEW-Compound **2**	−8.1
6B3J-Compound **2**	−8.8
5VAI-Compound **3**	−7.5
5VEW-Compound **3**	−7.9
6B3J-Compound **3**	−7.9
5VAI-Compound **4**	−8.5
5VEW-Compound **4**	−8.6
6B3J-Compound **4**	−9.2

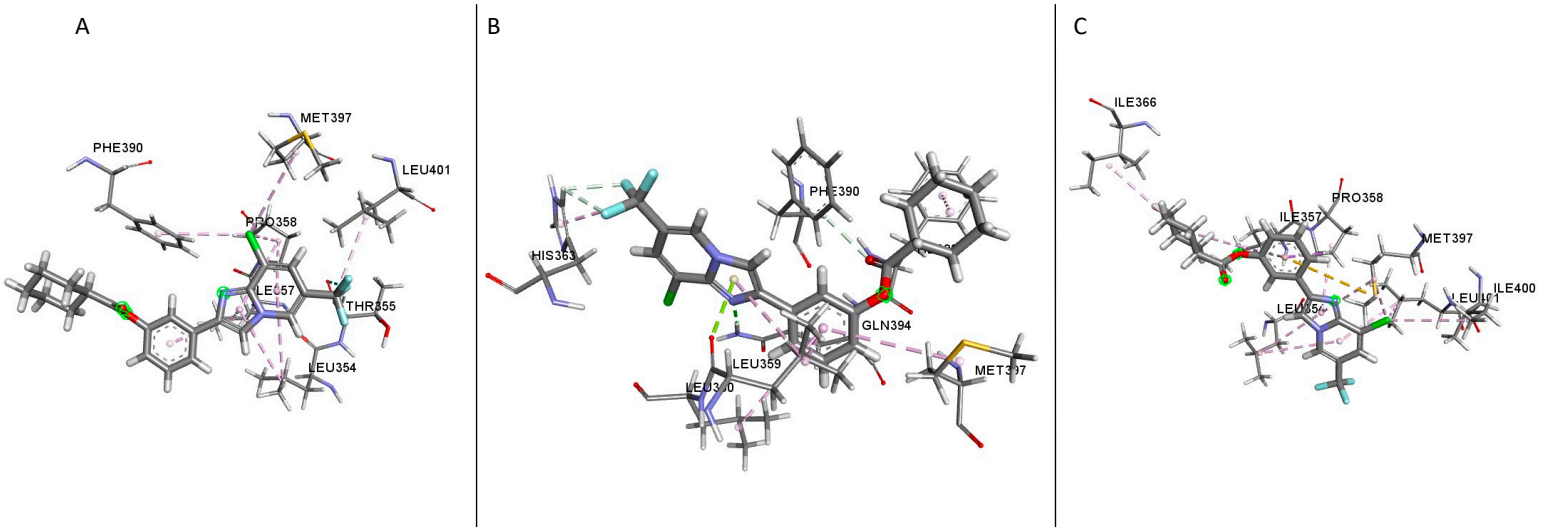

Figure 10. Schematic showing the ligands bound to the crystal structures of GLP-1R and the residues present in the active site. (**A**) 4:5VAI, (**B**) 4:5VEW, (**C**) 4:6B3J.

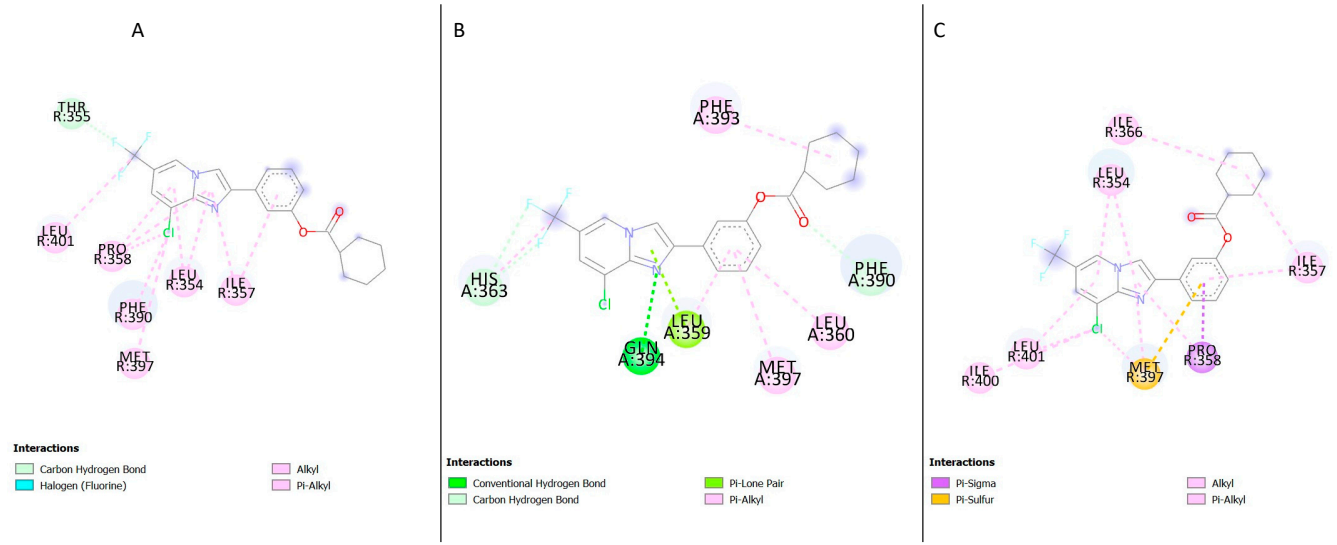

Figure 11. The protein–ligand interaction between compound **4** and the GLP 1 receptor generated using Schrodinger Maestro. (**A**) 4:5VAI (**B**) 4:5VEW and (**C**) 4:6B3J.

3.6. In Silico ADME/Tox Prediction

The findings of the in silico ADME/Tox evaluation of the allosteric modulators of GLP-1R are shown in the tables below. Table 6 shows the physicochemical properties of the selected allosteric modulators used for the study, including the following parameters: the octanol–water partition coefficient based on Moriguchi's model (MlogP), the octanol–water partition coefficient based on Simulation plus's model (SlogP), the octanol–water partition coefficient as a function of pH (logD), the predicted human jejunal permeability (peff), the blood-brain barrier filter (BBB filter), aqueous solubility in pure water (Sw), volume of distribution (VD), Lipinski's rule of 5 (Ro5), topological polar surface area (TPSA), hydrogen bond acceptors (HBA), hydrogen bond donors (HBD) and molecular weight (g/mol) (MW).

Table 6. Physicochemical properties of the selected allosteric modulators generated using ADMET Predictor 9.5.

Lig.	MW	MlogP	SlogP	logD	P_{eff} cm/s $\times 10^4$	BBB Filter	Sw mg/mL	VD L/kg	% Unbound	Ro5	TPSA	HBA	HBD
1	301.48	3.15	4.25	4.25	8.86	High	0.001	4.75	8.00	0	25.78 Å^2	5	0
2	458.59	3.39	4.42	4.42	1.75	High	0.0002	0.86	7.03	0	126.75 Å^2	6	0
3	340.75	3.37	5.08	5.08	8.15	High	0.0002	2.99	3.34	0	51.08 Å^2	5	0
4	422.83	4.34	6.43	6.43	4.27	High	4.5×10^{-5}	3.48	2.79	1	43.60 Å^2	6	0

The results of the effects of the allosteric modulators on transport proteins predicted in silico are presented in Table 7. Table 8 shows the results of the activity of the allosteric modulators on the various isoforms of hepatic CYP450. Table 9 shows the toxicity parameters predicted using ADMET Predictor 9.5.

Table 7. Effect of the selected allosteric modulators generated using ADMET Predictor 9.5 on transport proteins.

Lig.	Pgp Substrate	Pgp Inhibitor	OATP1B1 Inhibitor	OCT2 Inhibitor	BSEP Inhibitor	BCRP Substrate
1	No	No	No	Yes	No	Yes
2	No	Yes	No	Yes	Yes	No
3	No	No	No	Yes	Yes	Yes
4	No	Yes	No	Yes	Yes	Yes

Table 8. Predicted metabolism of the selected allosteric modulators via cytochrome P450 isoforms.

Lig.	CYP1A2	CYP2A6	CYP2B6	CYP2C8	CYP2C9	CYP2C19	CYP2D6	CYP2E1	CYP3A4
1	+/-	+	+	NS	NI/+	NI/+	NI/NS	+	NI/+
2	-/NS	NS	NS	+	-/NS	NI/NS	-/NS	NS	+/-
3	+/-	+	+	NS	NI/+	NI/+	NI/+	NS	NI/+
4	-/NS	NS	NS	NS	-/NS	-/NS	NI/NS	NS	NI/+

Key; Inhibition of CYP isoform: (-), substrate of CYP isoform: (+), NS = Non-substrate, NI = Non-inhibitor.

Table 9. Toxicity parameters predicted using ADMET Predictor 9.5.

Lig.	AMES Toxicity	Skin Sens	hERG Filter	Repro Tox	Ser AlkPhos	Ser GGT	Ser AST	Ser ALT
1	Negative	+	No	Non-Toxic	Elevated	Elevated	Elevated	Elevated
2	Negative	-	No	Toxic	Elevated	Normal	Normal	Normal
3	Negative	+	No	Toxic	Elevated	Elevated	Elevated	Elevated
4	Negative	+	No	Toxic	Normal	Normal	Elevated	Elevated

Key; Sensitizer: (+), non-sensitizer: (-).

4. Discussion

Recent work has shown that T2D treatment needs the positive allosteric modulation of GLP-1R to inhibit glucagon secretion, thus stimulating insulin secretion [16]. It has also been suggested that the novel agonist human monoclonal antibody IRAB-A binds allosterically to the insulin receptor and thereby activates and enhances the signalling of insulin [27]. We demonstrate an application of these techniques in identifying the interactions occurring at the allosteric binding site of the GLP-1R using known allosteric modulators of GLP-1R. We also carried out in silico ADME/Tox evaluations of the compounds used in this study. Molecular docking is a virtual screening method used to discover new ligands for GPCRs, it should rank active molecules high and produce poses which will inform chemists which compounds to purchase for further screening [28].

Molecular docking has been used extensively in GPCR drug discovery to identify compounds (hit and lead generation) which target different receptors in the GPCR family [29]. Jenkins et al., utilised Flare to study 2-mercaptoacetamide (2MA) a structural analogue of urea, their findings showed that 2-MA is a competitive inhibitor and flare is a robust software for performing docking simulations [30]. Egorov et al., in their in silico docking study performed using flare showed that the synthesised compounds would play a significant role in the treatment of ailments such as breast cancer, neurodegenerative diseases etc [31]. Carlsson et al., applied molecular docking to perform a screening of over six million commercially available compounds against the active like conformations of $A_{2A}AR$. Their findings showed that nine of the 20 predicted agonists were confirmed to be $A_{2A}AR$ ligands [32]. Docking based programs can generate 3D conformations of binding structures which is very useful for function and drug-based analysis [33]. Hou et al., used techniques such as homology, molecular dynamics, and molecular docking to access prediction accuracy of ligand-binding poses and screening power of docking-based virtual screening. Their findings showed that the crystal structures outperformed the homology models before any refinement through molecular dynamics. However, the optimised homology models show a similar performance to the crystal structures following a docking assessment [34]. Shoichet et al., applied ligand docking to screen a large library of compounds to identify compounds with joint activity against on-targets and selectivity versus anti-targets using selected GPCRs (dopamine D_2, serotonin 5-HT_{2A}, histamine H_1, κ-opioid and μ-opioid receptors) [35]. Their findings showed a hit range of 40% to 65% for the on-targets with very reliable calculated binding affinities [35]. Docking into a crystal structure produces an accurate ligand binding pose prediction without any refinement [36]. The widescale application of molecular docking in drug development makes it a preferred method for this study; this has been paired with binding affinity predictions to determine the feasibility of the complexes.

The conformational transitions observed from the inactive to the active structures were similar to the findings of Liang et al. [20] who reported that the movement of TM 6 in the inactive state upon signalling created a binding pocket. The docking of the ligands to the inactive structure (PDB ID: 5VEW) is corroborated by Song et al. [16]; they reported that positive allosteric modulators (PAM) of the GLP-1R bind outside helices 5–7 near the intracellular part of the receptor, but in a distinct sub-pocket between helices 5 and 6.

The docking result of compound **1** showed several residues present in the binding sites of the different GLP-1R crystal structures; in the structure 5VAI, the following residues were identified (Table 1); Leu354, Lys351, Leu401, Thr355, Met397, Pro355, Phe390, Ile357 and Pro358 (Figure 5A). Most of these residues were hydrophobic amino acids except for Thr355 and Lys351; both are polar and positively charged, respectively. In the inactive structure 5VEW, the following residues were present in the binding site (Table 1), Arg348, Tyr402, Val405, Lys351, Leu349 and His180 (Figure 5B, Table 1). All the residues present in the binding site were polar. Upon examination of the structure 6B3J, the following residues interacted in the binding site (Table 1); Leu354, Ile357, Gln394, His363, Phe393, Met397, Pro358 and Phe390 (Figure 5C, Table 1). His363 and Gln394 were polar, while the remaining residues were hydrophobic. An analysis of the ligand's second and third top poses and

the protein structures showed the residues Thr355 and Leu401 were present in the first three poses of the 5VAI-Compound **1** complex (Tables 1, S2 and S3). The other protein structures used in the study did not have any similar interacting residues across the three poses analysed.

The presence of polar residues in the binding sites of the three structures examined suggests that these polar residues play a vital role in ligand binding [20]. The presence of these polar residues in the crystal structures of the receptor indicates the presence of a significant polar binding network around the peptide bindings site [20]. Bueno et al. [18] reported the capability of 2,6,7-trichloro-3-(trifluoromethyl)quinoxaline to potentiate GLP-1(9–36)-NH2-mediated cAMP accumulation in GLP-1R-expressing cells. The study results showed that compound **1** potentiated the activity of GLP-1(9–36)-NH2 on the wild-type receptor but failed to exert the same effect in cells expressing the mutant GLP-1R, which lacks the cysteine-347 residue [18]. A comparative molecular dynamics simulation showed that the cysteine-3476.36bF (C3476.36bF) mutant maximises van der Waals interactions with all the three negative allosteric modulators (NAMs) PF-06372222, NNC0640 and MK-0893 through the stabilisation of the aliphatic side chain of Lysine-3516.40b (K3516.40b) in an optimal conformation for hydrophobic interactions with NAMs [16,21]. An analysis of the findings from this study showed the residue Lys351(K351) forming hydrogen bonds and pi-cation interactions (Figure 5A,B and Figure 7B). The mutation S352→A terminates the inhibition of GLP-1R by NAMs while the T355→A eliminates the inhibition by NAMs, NNC0640 and PF-06372222 but doesn't inhibit the activity of MK-0893 [16]. The findings from previous research stated that positions 352–355 play a crucial role in binding an allosteric inhibitor to GLP-1R [16].

The examination of the docking results of compound **2** and the GLP-1R structures demonstrated several residues present in the active site of the crystal structures. In the active structure 5VAI, the following hydrophobic residues were present in the active site; Met397, Ile357, Leu354, Phe390. Thr355 was identified as the polar residues (Table 2, Figure 7A). All the residues interacting with the ligand in the binding site of the inactive crystal structure 5VEW were hydrophobic (Table 2, Figure 7B). Three of the residues, namely: Tyr402, His180 and Arg176 identified in the binding site of 6B3J, were polar, whilst the other residues were hydrophobic (Table 2, Figure 7C). The amino acid residue Phe390 interacted with compound **2**, and the structure 5VAI in the top three poses was analysed (Tables 2, S5 and S6). The analysis of the top three poses of the compound **2**-5VEW complex showed the amino acid residues Phe324, Leu354 and Pro 358 present in all the poses analysed (Tables 2, S5 and S6).

The presence of polar residues in the binding site of the GLP-1R crystal structures suggests critical hydrogen bond interactions which maintain receptor integrity and apo state [20]. A previous study has demonstrated the capacity of compound **2** to potentiate GLP-1(9–36)-NH2-mediated cAMP accumulation in GLP-1R-expressing cells. The study showed that compound **2** potentiated the activity of GLP-1(9–36)-NH2 on the wild-type receptor but failed to exert the same effect in cells expressing the mutant GLP-1R, which lacks the Cysteine-347 residue [18].

In the active structure (PDB ID: 5VAI [19]-Compound **3** complex), eight residues were identified in the active site, most of which were hydrophobic residues. The active site consists of hydrophobic residues Val327, Val331, Leu251, Leu255, Leu356, and Leu349. Thr353 and Ser352 are the residues responsible for the polar region of the binding site (Table 3, Figure 9A). Upon examination of the inactive structure (PDB ID: 5VEW [16]), there was an uneven distribution of polar (Tyr402, Asn407, His180, Arg348 and Lys351) and hydrophobic (Leu401 and Val405) amino acid residues (Table 3, Figure 9B). The active site of the other structure (PDB ID: 6B3J [20]) examined had the majority of hydrophobic residues present (Ile357, Phe393, Ile356, Pro358, Phe390, Met397) while the remaining residues (His363, Gln394) were polar (Table 3, Figure 9C). The presence of polar residues in the active sites of the structures examined implies a critical hydrogen bonding between the ligand and the residues [20].

An earlier study carried out by Gong et al. [37], reported that compounds which possess a 3-(8-chloro-6-(trifluoromethyl)imidazo[1,2-a]pyridine2-yl)phenyl acetate moiety, including compound **3** (3-(8-chloro-6-(trifluoromethyl)imidazo[1,2-a]pyridine-2-yl) phenylcyclo propane carboxylate), are selective GLP-1R agonists, and have potential as anti-diabetic treatment agents.

In the active structure (PDB ID: 5VAI [19]), seven residues were found in the compound **4** binding site; the majority of the residues were hydrophobic except Thr355 (Figure 11A). The docking result of the inactive structure (PDB ID: 5VEW [16]) showed the majority of the residues found in the active site being hydrophobic (Table 4, Figure 11B), His363 and Gln394 were the only polar residues identified in the binding site. Examination of the docking results with the crystal structure 6B3J (PDB ID: 6B3J [20]) showed that the residues interacting with the ligand were hydrophobic (Table 4, Figure 11C).

In a study carried out by Gong et al. [37], with screened heterocyclic small molecules, they discovered a novel skeleton of 3-(8-chloro-6-(trifluoromethyl)imidazo[1,2-a]pyridine2-yl)phenyl acetate derivative (compound **4**), which on further characterisation proved to be selective GLP-1R agonists which potentially had a therapeutic effect on diabetes. In a later study, performed by Bueno et al. [18], their findings inferred that compound **4** failed to activate GLP-1R through a covalent mechanism as it remained unaltered after 2 h and thus was considered non-reactive. An analysis of the top three binding poses of the all the protein–ligand complexes showed that the residues interacting with the ligands were slightly different albeit docking at TM6 for most of the poses (Tables 1–4 and S3–S10). This however would suggest a flexibility of the ligand within the binding pocket of the receptor.

The binding affinity (ΔG_{noelec}) values for the 5VAI-Compound **1**, 5VEW-Compound **1**, 6B3J-Compound **1**, 5VAI-Compound **2**, 5VEW-Compound **2**, 6B3J-Compound **2**, 5VAI-Compound **3**, 5VEW-Compound **3**, 6B3J-Compound **3**, 5VAI-Compound **4**, 5VEW-Compound **4**, 6B3J-Compound **4** was revealed to be −6.8 Kcal/mol, −7.2 Kcal/mol, −7.2 Kcal/mol, −8.5 Kcal/mol, −8.1 Kcal/mol, −8.8 Kcal/mol, −7.5 Kcal/mol, −7.9 Kcal/mol, −7.9 Kcal/mol, −8.5 Kcal/mol, −8.6 Kcal/mol, −9.2 Kcal/mol respectively (Table 5). The results showed that the dockings were feasible energetically; this was demonstrated by the negative Gibbs free energy (ΔG) values (Table 5). The findings showed that compound **4**-protein structure (PDB IDs: 5VAI [19], 6B3J [20], 5VEW [16]) complexes had the highest predicted binding affinities. This suggests that compound **4** would be bound tightly to the allosteric binding site of the receptor. The findings on Table 5, also show that compound **2** and compound **4** would be bound strongly to the allosteric binding site of the GLP-1R.

The in silico prediction of ADME/Tox properties of any new drug candidate is essential in drug development, thus allowing scientists to investigate its properties to optimise the drug candidates to acceptable ADME/Tox standards [38]. The findings in Table 6 showed that the allosteric modulators complied with Lipinski's rule of five except compound **4**. According to the ADMET Predictor software, compound **4** violated the rule because of a high logP value of over 5.6. This translates to compound **4** not being a likely drug candidate according to the traditional method of evaluating drug-likeness; Lipinski's rule of 5. The molecular descriptors HBA and HBD were found to comply with the cut off limits of Ro5 (Table 6). The ligands evaluated in this study complied with the Veber drug-likeness filter (rotatable bonds ≤ 10, TPSA ≤ 140) [39]. Based on the rule of three for fragment-based drug discovery (molecular weight < 300, ClogP < 3, the number of hydrogen bond donors and acceptors < 3 and the number of rotatable bonds < 3), the ligands violated all the rules [40]. Lipophilicity is often expressed as the distribution coefficient in water/octanol (logD); this parameter influences some processes like plasma protein binding, oral absorption and VD [41]. Nevertheless, higher logD values translate to higher vulnerability to P450 metabolism leading to higher clearance [41]. The predicted logD values presented in Table 5 showed compound **4** with the highest logD value while compound **1** had the least. However, all the ligands also possessed high logD values of over 3.5 which leads to low aqueous solubility, this makes these ligands potentially promiscuous as high lipophilicity often leads to low metabolic clearance and toxicity. The predicted human jejunal permeability (P_{eff})

values (Table 6) show that the allosteric modulators had values of over 1.5 cm/s $\times$ 10^4; this indicates that the allosteric modulators would be absorbed entirely. This finding is corroborated by previous research, which reports that drug candidates with a P_{eff} value of >1.5 would be wholly absorbed irrespective of transport mechanism(s) being utilised [42].

The volume of distribution (VD) is essential in ADME studies [43]. It relates to the amount of a drug in the body to the measured concentration in a suitable biological fluid [43]. The findings for the VD parameter (Table 6) showed compound **2** having the lowest value (0.86 L/kg) while compound **1** had the highest. Hassan et al. reported that VD values of <5.5 L/kg guaranteed decreased deep tissue penetration [44]. Nonetheless, compounds that enter tissues and bind extensively will show VD above the total body water (i.e., any value greater than 1 L/kg) [45]. The allosteric modulators would remain in the bloodstream for an extended period, thus exerting their effects over a longer period due to their predicted high plasma protein binding (% unbound) of over 90% (Table 6). The ADME/Tox software predicted high BBB penetration for all the allosteric modulators investigated. This implies that the allosteric modulators investigated may potentially treat ailments affecting the brain (Table 6). The predicted TPSA values (Table 6) shows compounds **1**, **3** and **4** with TPSA values of less than 60 Å^2, while the compound **2** TPSA value was above 60 Å^2 but less than 140 Å^2. In 2009, Fernandes and Gattass [46] reported that molecules with PSA values greater than 140 Å^2 are believed to have low cell membrane penetrating capacity, while those with PSA $\leq$ 60 Å^2 are easily absorbed.

All the allosteric modulators investigated were not substrates of P-glycoprotein (P-gp); compound **3** and compound **4** were identified as inhibitors of P-gp (Table 7). Even though most compounds do not inhibit P-gp, there is a possibility that the allosteric modulators can be transported out of the cell by it [47]. The allosteric modulators were not inhibitors of organic anion transporting polypeptide 1B1 (OATP1B1), but the prediction showed that the allosteric modulators were inhibitors of organic cation transporter 2 (OCT2) (Table 7). All the ligands inhibited bile salt export pump (BSEP) except compound **1**, while the rest were substrates of breast cancer resistance protein (BCRP) except the allosteric modulator compound **3**. Cytochrome P450 (CYP450) are the enzymes that catalyse the oxidation of organic substances [44]. The evaluation of the allosteric modulators on the various isoforms of hepatic CYP450 was also predicted; the findings are shown in Table 8. Table 8 demonstrates that all the allosteric modulators were substrates of CYP3A4, albeit compound **3** was an isoform inhibitor. Allosteric modulators showed inhibitory tendencies and substrate specificities for the various isoforms investigated (Table 8). The ADMET predictor software inferred that the clearance pathway for the allosteric modulators studied is via metabolism. Drug toxicity has resulted in the failure of drug candidates in clinical trials, hence, the use of in silico models to predict the potential toxicity of new drug candidates [43].

The predicted toxicity parameters were shown in Table 9; all allosteric modulators evaluated reported negative for AMES toxicity. The hERG filter parameter returned negative, implying that the allosteric modulators do not have an affinity for the hERG potassium channel in humans. All the allosteric modulators studied could cause potential reproductive/developmental toxicity except compound **1** (Table 9). The allosteric modulators were all skin sensitisers except compound **3** (Table 9). The liver function parameters (Table 9) showed some of the allosteric modulators causing elevations in levels of liver enzymes studied. Compound **1** and compound **2** elevated the levels of the liver functions studied (Table 9), resulting in them being classed as hepatotoxic by the prediction software.

5. Conclusions and Future Directions

The glucagon-like peptide 1 receptor (GLP-1R) is a member of the family (or class) B G-protein-coupled receptor (GPCR). The receptor is a regulator of insulin and a key target in treating Type 2 diabetes mellitus. In this research, computational chemistry techniques such as molecular docking were combined with in silico ADME/Tox predictions to determine the position and structure of the allosteric binding site, as well as to examine how the

allosteric modulators bind to the binding site. In silico evaluation was used to evaluate the ADME/Tox properties of the allosteric modulators.

The allosteric modulators (compounds **1**, **2**, **3** and **4**) used in the study docked at various positions across TM5, TM6 and TM7 in both the active and inactive structures. Based on these findings, it can be inferred that the allosteric binding site is situated around TM6 of the receptor. Analysis of the top three binding poses of the all the protein–ligand complexes showed that the residues interacting with the ligands were slightly different even though the ligands docked at TM6 for most of the poses (Tables 1–4 and Tables S3–S10). This however would suggest a flexibility of the ligand within the binding pocket of the receptor. The results of the research are in line with the findings of a previous study. It was reported that positive and negative allosteric modulators of GLP-1R bind to the same region just outside TM5-TM7 near the intracellular section of the receptor [16]. However, the PAMs bind in a well-defined sub-pocket at the interface between TM5 and TM6, thus facilitating the formation of an intracellular binding site that enhances G-protein coupling [16]. Further mutagenesis studies need to be carried to understand which residues play a significant role in ligand binding.

The binding analysis showed that the dockings were feasible energetically; this was demonstrated by the negative Gibbs free energy (ΔG) values (Table 5). The findings showed that compound **4**-protein structure (PDB IDs: 5VAI [19], 6B3J [20], 5VEW [16]) complexes had the highest predicted binding affinities. The binding affinity results suggest that compound **4** may be an agonist of the receptor, a biased agonist or perhaps an antagonist of the receptor because of its high in silico predicted binding affinity. This needs to be further characterised experimentally using assays such as radioligand binding assay or fluorescent ligand binding assay.

The ADMET predictions of the allosteric modulators studied showed the compounds possessing drug-like properties, except for compound **4** due to its high LogP value. The predicted human jejunal permeability (P_{eff}) values (Table 6) show that the allosteric modulators had over 1.5 cm/s $\times$ 10^4. This indicates that the allosteric modulators would be absorbed entirely. The predicted TPSA values (Table 6) shows compounds **1**, **3** and **4** with TPSA values of less than 60 Å^2, while the compound **2** TPSA value was above 60 Å^2 but less than 140 Å^2. These findings were corroborated by research carried out by Fernandes and Gattass in 2009 [46] and Wang et al. in 2014 [42]. The ADME predictions of the compounds presented showed that these all have high LogD values and low aqueous solubility. High lipophilicity often leads low metabolic clearance and toxicity.

Conclusively, docking simulations provide insights into potential allosteric binding sites and possible interactions. The results of an in silico ADME/Tox study are essential in developing a potential drug candidate. Further studies could be carried out using known allosteric modulators sourced from a literature search to characterise the allosteric binding pocket of GLP-1R further using molecular dynamics (MD) simulations [48–51], and multi-scale quantum mechanics (QM)/molecular mechanics (MM) molecular simulations [52].

Supplementary Materials: The following are available online at https://www.mdpi.com/article/10.3390/applbiosci1020010/s1, Table S1. Table showing the GPCR crystal structures resolved between 2017 and 2021; Table S2. The binding energy of the ligands upon docking onto the crystal structures studied; Table S3. Table showing amino acids present in the binding sites for compound **1** Pose 2; Table S4. Table showing amino acids present in the binding sites for compound **1** Pose 3; Table S5. Table showing amino acids present in the binding sites for compound **2** Pose 2; Table S6. Table showing amino acids present in the binding sites for compound **2** Pose 3; Table S7. Table showing amino acids present in the binding sites for compound **3** Pose 2; Table S8. Table showing amino acids present in the binding sites for compound **3** Pose 3; Table S9. Table showing amino acids present in the binding sites for compound **4** Pose 2; Table S10. Table showing amino acids present in the binding sites for compound **4** Pose 3. References [21–23,53–62] are cited in the supplementary materials.

Author Contributions: Conceptualization, P.B.W. and Z.A.; methodology, J.S. and P.B.W.; software, M.M.; validation, C.S.O., M.-W.C. and B.P.; formal analysis, C.S.O.; investigation, M.M.; resources, S.C.L.K.; writing—review and editing, S.C.L.K., I.H.W. and P.B.W.; visualization, M.M.; supervision, E.H., Z.A., S.C.L.K. and P.B.W.; project administration, E.H.; funding acquisition, P.B.W. All authors have read and agreed to the published version of the manuscript.

Funding: This research received no external funding.

Institutional Review Board Statement: Not applicable.

Informed Consent Statement: Not applicable.

Data Availability Statement: The data presented in this study are available on request from the corresponding author. The data are not publicly available due to the nature of the datasets contained herein and their relative size.

Conflicts of Interest: The authors declare no conflict of interest.

References

1. Lagerström, M.C.; Schiöth, H.B. Structural diversity of G protein-coupled receptors and significance for drug discovery. *Nat. Rev. Drug Discov.* **2008**, *7*, 339–357. [CrossRef] [PubMed]
2. Karageorgos, V.; Venihaki, M.; Sakellaris, S.; Pardalos, M.; Kontakis, G.; Matsoukas, M.-T.; Gravanis, A.; Margioris, A.; Liapakis, G. Current understanding of the structure and function of family B GPCRs to design novel drugs. *Hormones* **2018**, *17*, 45–59. [CrossRef] [PubMed]
3. de Graaf, C.; Song, G.; Cao, C.; Zhao, Q.; Wang, M.-W.; Wu, B.; Stevens, R.C. Extending the Structural View of Class B GPCRs. *Trends Biochem. Sci.* **2017**, *42*, 946–960. [CrossRef] [PubMed]
4. Pándy-Szekeres, G.; Munk, C.; Tsonkov, T.M.; Mordalski, S.; Harpsøe, K.; Hauser, A.S.; Bojarski, A.J.; Gloriam, D.E. GPCRdb in 2018: Adding GPCR structure models and ligands. *Nucleic Acids Res.* **2018**, *46*, D440–D446. [CrossRef] [PubMed]
5. Kooistra, A.J.; Mordalski, S.; Pándy-Szekeres, G.; Esguerra, M.; Mamyrbekov, A.; Munk, C.; Keserű, G.M.; Gloriam, D.E. GPCRdb in 2021: Integrating GPCR sequence, structure and function. *Nucleic Acids Res.* **2021**, *49*, D335–D343. [CrossRef]
6. Zhang, J.; Gu, S.; Sun, X.; Li, W.; Tang, Y.; Liu, G. Computational insight into conformational states of glucagon-like peptide-1 receptor (GLP-1R) and its binding mode with GLP-1. *RSC Adv.* **2016**, *6*, 13490–13497. [CrossRef]
7. Bodnaruc, A.M.; Prud'homme, D.; Blanchet, R.; Giroux, I. Nutritional modulation of endogenous glucagon-like peptide-1 secretion: A review. *Nutr. Metab.* **2016**, *13*, 92. [CrossRef]
8. Sharma, R.; McDonald, T.S.; Eng, H.; Limberakis, C.; Stevens, B.D.; Patel, S.; Kalgutkar, A.S. In Vitro Metabolism of the Glucagon-Like Peptide-1 (GLP-1)–Derived Metabolites GLP-1(9–36)amide and GLP-1(28–36)amide in Mouse and Human Hepatocytes. *Drug Metab. Dispos.* **2013**, *41*, 2148. [CrossRef]
9. Li, J.; Zheng, J.; Wang, S.; Lau, H.K.; Fathi, A.; Wang, Q. Cardiovascular Benefits of Native GLP-1 and its Metabolites: An Indicator for GLP-1-Therapy Strategies. *Front. Physiol.* **2017**, *8*, 15. [CrossRef]
10. Taing, M.-W.; Rose, F.J.; Whitehead, J.P. GLP-1(28–36)amide, the Glucagon-like peptide-1 metabolite: Friend, foe, or pharmacological folly? *Drug Des. Dev. Ther.* **2014**, *8*, 677–688. [CrossRef]
11. Tomas, E.; Habener, J.F. Insulin-like actions of glucagon-like peptide-1: A dual receptor hypothesis. *Trends Endocrinol. Metab. TEM* **2010**, *21*, 59–67. [CrossRef]
12. Holst, J.J. The Physiology of Glucagon-like Peptide 1. *Physiol. Rev.* **2007**, *87*, 1409–1439. [CrossRef]
13. Donnelly, D. The structure and function of the glucagon-like peptide-1 receptor and its ligands. *Br. J. Pharmacol.* **2012**, *166*, 27–41. [CrossRef]
14. Athauda, D.; Foltynie, T. The glucagon-like peptide 1 (GLP) receptor as a therapeutic target in Parkinson's disease: Mechanisms of action. *Drug Discov. Today* **2016**, *21*, 802–818. [CrossRef]
15. Ahrén, B. GLP-1 for type 2 diabetes. *Exp. Cell Res.* **2011**, *317*, 1239–1245. [CrossRef]
16. Song, G.; Yang, D.; Wang, Y.; de Graaf, C.; Zhou, Q.; Jiang, S.; Liu, K.; Cai, X.; Dai, A.; Lin, G.; et al. Human GLP-1 receptor transmembrane domain structure in complex with allosteric modulators. *Nature* **2017**, *546*, 312–315. [CrossRef]
17. Schiöth, H.B.; Fredriksson, R. The GRAFS classification system of G-protein coupled receptors in comparative perspective. *Gen. Comp. Endocrinol.* **2005**, *142*, 94–101. [CrossRef]
18. Bueno, A.B.; Showalter, A.D.; Wainscott, D.B.; Stutsman, C.; Marín, A.; Ficorilli, J.; Cabrera, O.; Willard, F.S.; Sloop, K.W. Positive Allosteric Modulation of the Glucagon-like Peptide-1 Receptor by Diverse Electrophiles. *J. Biol. Chem.* **2016**, *291*, 10700–10715. [CrossRef]
19. Zhang, Y.; Sun, B.; Feng, D.; Hu, H.; Chu, M.; Qu, Q.; Tarrasch, J.T.; Li, S.; Sun Kobilka, T.; Kobilka, B.K.; et al. Cryo-EM structure of the activated GLP-1 receptor in complex with a G protein. *Nature* **2017**, *546*, 248–253. [CrossRef] [PubMed]
20. Liang, Y.-L.; Khoshouei, M.; Glukhova, A.; Furness, S.G.B.; Zhao, P.; Clydesdale, L.; Koole, C.; Truong, T.T.; Thal, D.M.; Lei, S.; et al. Phase-plate cryo-EM structure of a biased agonist-bound human GLP-1 receptor–Gs complex. *Nature* **2018**, *555*, 121–125. [CrossRef]

21. Xu, Y.; Wang, Y.; Liu, K.; Peng, Y.; Yao, D.; Tao, H.; Liu, H.; Song, G. Mutagenesis facilitated crystallization of GLP-1R. *IUCrJ* **2019**, *6*, 996–1006. [CrossRef] [PubMed]
22. Bueno, A.B.; Sun, B.; Willard, F.S.; Feng, D.; Ho, J.D.; Wainscott, D.B.; Showalter, A.D.; Vieth, M.; Chen, Q.; Stutsman, C.; et al. Structural insights into probe-dependent positive allosterism of the GLP-1 receptor. *Nat. Chem. Biol.* **2020**, *16*, 1105–1110. [CrossRef] [PubMed]
23. Kawai, T.; Sun, B.; Yoshino, H.; Feng, D.; Suzuki, Y.; Fukazawa, M.; Nagao, S.; Wainscott, D.B.; Showalter, A.D.; Droz, B.A.; et al. Structural basis for GLP-1 receptor activation by LY3502970, an orally active nonpeptide agonist. *Proc. Natl. Acad. Sci. USA* **2020**, *117*, 29959–29967. [CrossRef]
24. Vangone, A.; Schaarschmidt, J.; Koukos, P.; Geng, C.; Citro, N.; Trellet, M.E.; Xue, L.C.; Bonvin, A.M.J.J. Large-scale prediction of binding affinity in protein–small ligand complexes: The PRODIGY-LIG web server. *Bioinformatics* **2019**, *35*, 1585–1587. [CrossRef]
25. Kurkcuoglu, Z.; Koukos, P.I.; Citro, N.; Trellet, M.E.; Rodrigues, J.; Moreira, I.S.; Roel-Touris, J.; Melquiond, A.S.J.; Geng, C.; Schaarschmidt, J. Performance of HADDOCK and a simple contact-based protein–ligand binding affinity predictor in the D3R Grand Challenge 2. *J. Comput.-Aided Mol. Des.* **2018**, *32*, 175–185. [CrossRef]
26. Kar, T.; Narsaria, U.; Basak, S.; Deb, D.; Castiglione, F.; Mueller, D.M.; Srivastava, A.P. A candidate multi-epitope vaccine against SARS-CoV-2. *Sci. Rep.* **2020**, *10*, 10895. [CrossRef]
27. Hinke, S.A.; Cieniewicz, A.M.; Kirchner, T.; D'Aquino, K.; Nanjunda, R.; Aligo, J.; Perkinson, R.; Cooper, P.; Boayke, K.; Chiu, M.L.; et al. Unique pharmacology of a novel allosteric agonist/sensitizer insulin receptor monoclonal antibody. *Mol. Metab.* **2018**, *10*, 87–99. [CrossRef]
28. Weiss, D.R.; Bortolato, A.; Tehan, B.; Mason, J.S. GPCR-Bench: A Benchmarking Set and Practitioners' Guide for G Protein-Coupled Receptor Docking. *J. Chem. Inf. Model.* **2016**, *56*, 642–651. [CrossRef]
29. Congreve, M.; de Graaf, C.; Swain, N.A.; Tate, C.G. Impact of GPCR Structures on Drug Discovery. *Cell* **2020**, *181*, 81–91. [CrossRef] [PubMed]
30. Milo, S.; Heylen, R.A.; Glancy, J.; Williams, G.T.; Patenall, B.L.; Hathaway, H.J.; Thet, N.T.; Allinson, S.L.; Laabei, M.; Jenkins, A.T.A. A small-molecular inhibitor against Proteus mirabilis urease to treat catheter-associated urinary tract infections. *Sci. Rep.* **2021**, *11*, 3726. [CrossRef] [PubMed]
31. Ryzhkova, Y.E.; Elinson, M.N.; Vereshchagin, A.N.; Karpenko, K.A.; Ryzhkov, F.V.; Ushakov, I.E.; Egorov, M.P. Multicomponent Electrocatalytic Selective Approach to Unsymmetrical Spiro[furo[3,2-c]pyran-2,5′-pyrimidine] Scaffold under a Column Chromatography-Free Protocol at Room Temperature. *Chemistry* **2022**, *4*, 615–629. [CrossRef]
32. Rodríguez, D.; Gao, Z.G.; Moss, S.M.; Jacobson, K.A.; Carlsson, J. Molecular docking screening using agonist-bound GPCR structures: Probing the A2A adenosine receptor. *J. Chem. Inf. Model.* **2015**, *55*, 550–563. [CrossRef] [PubMed]
33. Chan, W.K.B.; Zhang, Y. Virtual Screening of Human Class-A GPCRs Using Ligand Profiles Built on Multiple Ligand-Receptor Interactions. *J. Mol. Biol.* **2020**, *432*, 4872–4890. [CrossRef] [PubMed]
34. Chen, H.; Fu, W.; Wang, Z.; Wang, X.; Lei, T.; Zhu, F.; Li, D.; Chang, S.; Xu, L.; Hou, T. Reliability of Docking-Based Virtual Screening for GPCR Ligands with Homology Modeled Structures: A Case Study of the Angiotensin II Type I Receptor. *ACS Chem. Neurosci.* **2019**, *10*, 677–689. [CrossRef] [PubMed]
35. Weiss, D.R.; Karpiak, J.; Huang, X.-P.; Sassano, M.F.; Lyu, J.; Roth, B.L.; Shoichet, B.K. Selectivity Challenges in Docking Screens for GPCR Targets and Antitargets. *J. Med. Chem.* **2018**, *61*, 6830–6845. [CrossRef]
36. Loo, J.S.E.; Emtage, A.L.; Ng, K.W.; Yong, A.S.J.; Doughty, S.W. Assessing GPCR homology models constructed from templates of various transmembrane sequence identities: Binding mode prediction and docking enrichment. *J. Mol. Graph. Model.* **2018**, *80*, 38–47. [CrossRef]
37. Gong, Y.-D.; Cheon, H.-G.; Lee, T.; Kang, N.S. A Novel 3-(8-Chloro-6-(trifluoromethyl)imidazo[1,2-a]pyridine-2-yl)phenyl Acetate Skeleton and Pharmacophore Model as Glucagon-like Peptide 1 Receptor Agonists. *Bull. Korean Chem. Soc.* **2010**, *31*, 3760–3764. [CrossRef]
38. Akabli, T.; Lamchouri, F.; Senhaji, S.; Toufik, H. Molecular docking, ADME/Tox prediction, and in vitro study of the cell growth inhibitory activity of five β-carboline alkaloids. *Struct. Chem.* **2019**, *30*, 1495–1504. [CrossRef]
39. Veber, D.F.; Johnson, S.R.; Cheng, H.Y.; Smith, B.R.; Ward, K.W.; Kopple, K.D. Molecular properties that influence the oral bioavailability of drug candidates. *J. Med. Chem.* **2002**, *45*, 2615–2623. [CrossRef]
40. Jhoti, H.; Williams, G.; Rees, D.C.; Murray, C.W. The 'rule of three' for fragment-based drug discovery: Where are we now? *Nat. Rev. Drug Discov.* **2013**, *12*, 644–645. [CrossRef]
41. van de Waterbeemd, H.; Smith, D.A.; Jones, B.C. Lipophilicity in PK design: Methyl, ethyl, futile. *J. Comput.-Aided Mol. Des.* **2001**, *15*, 273–286. [CrossRef] [PubMed]
42. Wang, C.; Avdeef, A.; Zhang, W.; Tam, K.Y. Predicting the human jejunal permeability and fraction absorbed of fluoroquinolones based on a biophysical model. *Bio-Med. Mater. Eng.* **2014**, *24*, 3849–3854. [CrossRef]
43. Rashid, U.; Hassan, S.F.; Nazir, S.; Wadood, A.; Waseem, M.; Ansari, F.L. Synthesis, docking studies, and in silico ADMET predictions of some new derivatives of pyrimidine as potential KSP inhibitors. *Med. Chem. Res.* **2015**, *24*, 304–315. [CrossRef]
44. Hassan, S.F.; Rashid, U.; Ansari, F.L.; Ul-Haq, Z. Bioisosteric approach in designing new monastrol derivatives: An investigation on their ADMET prediction using in silico derived parameters. *J. Mol. Graph. Model.* **2013**, *45*, 202–210. [CrossRef]

45. Beaumont, K.; Cole, S.M.; Gibson, K.; Gosset, J.R. Chapter 2 ADMET for the Medicinal Chemist. In *Metabolism, Pharmacokinetics and Toxicity of Functional Groups: Impact of Chemical Building Blocks on ADMET*; The Royal Society of Chemistry: London, UK, 2010; pp. 61–98.
46. Fernandes, J.; Gattass, C.R. Topological Polar Surface Area Defines Substrate Transport by Multidrug Resistance Associated Protein 1 (MRP1/ABCC1). *J. Med. Chem.* **2009**, *52*, 1214–1218. [CrossRef]
47. Vukic, V.R.; Loncar, D.M.; Vukic, D.V.; Jevric, L.R.; Benedekovic, G.; Francuz, J.; Kojic, V.; Karadzic Banjac, M.Z.; Popsavin, V. In vitro antitumor activity, ADME-Tox and 3D-QSAR of synthesized and selected natural styryl lactones. *Comput. Biol. Chem.* **2019**, *83*, 107112. [CrossRef]
48. Mohammadi, M.; Mohammadiarani, H.; Shaw, V.S.; Neubig, R.R.; Vashisth, H. Interplay of cysteine exposure and global protein dynamics in small-molecule recognition by a regulator of G-protein signaling protein. *Proteins Struct. Funct. Bioinform.* **2019**, *87*, 146–156. [CrossRef]
49. Schuster, K.D.; Mohammadi, M.; Cahill, K.B.; Matte, S.L.; Maillet, A.D.; Vashisth, H.; Cote, R.H. Pharmacological and molecular dynamics analyses of differences in inhibitor binding to human and nematode PDE4: Implications for management of parasitic nematodes. *PLoS ONE* **2019**, *14*, e0214554. [CrossRef]
50. Renault, P.; Louet, M.; Marie, J.; Labesse, G.; Floquet, N. Molecular Dynamics Simulations of the Allosteric Modulation of the Adenosine A2a Receptor by a Mini-G Protein. *Sci. Rep.* **2019**, *9*, 5495. [CrossRef] [PubMed]
51. Vettoretti, G.; Moroni, E.; Sattin, S.; Tao, J.; Agard, D.A.; Bernardi, A.; Colombo, G. Molecular Dynamics Simulations Reveal the Mechanisms of Allosteric Activation of Hsp90 by Designed Ligands. *Sci. Rep.* **2016**, *6*, 23830. [CrossRef]
52. Nakliang, P.; Lazim, R.; Chang, H.; Choi, S. Multiscale Molecular Modeling in G Protein-Coupled Receptor (GPCR)-Ligand Studies. *Biomolecules* **2020**, *10*, 631. [CrossRef] [PubMed]
53. Jazayeri, A.; Rappas, M.; Brown, A.J.H.; Kean, J.; Errey, J.C.; Robertson, N.J.; Fiez-Vandal, C.; Andrews, S.P.; Congreve, M.; Bortolato, A.; et al. Crystal structure of the GLP-1 receptor bound to a peptide agonist. *Nature* **2017**, *546*, 254–258. [CrossRef] [PubMed]
54. Evers, A.; Bossart, M.; Pfeiffer-Marek, S.; Elvert, R.; Schreuder, H.; Kurz, M.; Stengelin, S.; Lorenz, M.; Herling, A.; Konkar, A.; et al. Dual Glucagon-like Peptide 1 (GLP-1)/Glucagon Receptor Agonists Specifically Optimized for Multidose Formulations. *J. Med. Chem.* **2018**, *61*, 5580–5593. [CrossRef]
55. Wu, F.; Yang, L.; Hang, K.; Laursen, M.; Wu, L.; Han, G.W.; Ren, Q.; Roed, N.K.; Lin, G.; Hanson, M.A.; et al. Full-length human GLP-1 receptor structure without orthosteric ligands. *Nat. Commun.* **2020**, *11*, 1272. [CrossRef]
56. Zhao, P.; Liang, Y.-L.; Belousoff, M.J.; Deganutti, G.; Fletcher, M.M.; Willard, F.S.; Bell, M.G.; Christe, M.E.; Sloop, K.W.; Inoue, A.; et al. Activation of the GLP-1 receptor by a non-peptidic agonist. *Nature* **2020**, *577*, 432–436. [CrossRef]
57. Zhang, X.; Belousoff, M.J.; Zhao, P.; Kooistra, A.J.; Truong, T.T.; Ang, S.Y.; Underwood, C.R.; Egebjerg, T.; Šenel, P.; Stewart, G.D.; et al. Differential GLP-1R Binding and Activation by Peptide and Non-peptide Agonists. *Mol. Cell* **2020**, *80*, 485–500. [CrossRef]
58. Ma, H.; Huang, W.; Wang, X.; Zhao, L.; Jiang, Y.; Liu, F.; Guo, W.; Sun, X.; Zhong, W.; Yuan, D.; et al. Structural insights into the activation of GLP-1R by a small molecule agonist. *Cell Res.* **2020**, *30*, 1140–1142. [CrossRef]
59. Cong, Z.; Chen, L.-N.; Ma, H.; Zhou, Q.; Zou, X.; Ye, C.; Dai, A.; Liu, Q.; Huang, W.; Sun, X.; et al. Molecular insights into ago-allosteric modulation of the human glucagon-like peptide-1 receptor. *Nat. Commun.* **2021**, *12*, 3763. [CrossRef]
60. Zhang, X.; Belousoff, M.J.; Liang, Y.-L.; Danev, R.; Sexton, P.M.; Wootten, D. Structure and dynamics of semaglutide- and taspoglutide-bound GLP-1R-Gs complexes. *Cell Rep.* **2021**, *36*, 109374. [CrossRef]
61. Zhang, X.; Johnson, R.M.; Drulyte, I.; Yu, L.; Kotecha, A.; Danev, R.; Wootten, D.; Sexton, P.M.; Belousoff, M.J. Evolving cryo-EM structural approaches for GPCR drug discovery. *Structure* **2021**, *29*, 963–974. [CrossRef]
62. Johnson, R.M.; Zhang, X.; Piper, S.J.; Nettleton, T.J.; Vandekolk, T.H.; Langmead, C.J.; Danev, R.; Sexton, P.M.; Wootten, D. Cryo-EM structure of the dual incretin receptor agonist, peptide-19, in complex with the glucagon-like peptide-1 receptor. *Biochem. Biophys. Commun.* **2021**, *578*, 84–90. [CrossRef] [PubMed]